Appl. Phys. B 80, 595–601 (2005)
DOI: 10.1007/s00340-004-1734-9

Applied Physics B
Lasers and Optics

R.A. GANEEV[1,2,✉]
M. BABA[1]
A.I. RYASNYANSKY[3]
M. SUZUKI[1]
H. KURODA[1]

Laser ablation of GaAs in liquids: structural, optical, and nonlinear optical characteristics of colloidal solutions

[1]The Institute for Solid State Physics, The University of Tokyo, 5-1-5 Kashiwanoha, Kashiwa, Chiba 277-8581, Japan
[2]NPO Akadempribor, Akademgorodok, Tashkent 700125, Uzbekistan
[3]Institut des Nano-Sciences de Paris, CNRS – Université Pierre et Marie Curie, Case 80, 140 rue de Lourmel, 75015 Paris, France

Received: 19 May 2004 / Revised version: 6 September 2004
Published online: 18 February 2005 •

ABSTRACT We investigated the optical, structural, and nonlinear optical properties of GaAs nanoparticles prepared by laser ablation in various liquids at the wavelengths of 795 nm and 1,054 nm. The slow-thermal-effect-induced self-defocusing processes were dominating both in the cases of high pulse repetition rate and nanosecond pulses. The two-photon absorption was observed in these colloidal solutions in the case of low pulse repetition rate of picosecond and femtosecond radiation. The nonlinear susceptibility of GaAs nanoparticles ablated in water was measured to be 2×10^{-9} esu.

PACS 42.65.An; 42.65.Jx; 42.70.Nq; 78.40.Fy; 78.67.Bf

1 Introduction

The semiconductor quantum dots, semiconductor nanoparticles-doped glasses, and colloidal microcrystallites have attracted extensive attention over the past decade [1]. In particular, the interest in GaAs nanoparticles was attributed to their potential applications in nonlinear optics. The analysis of nonlinear optical characteristics of bulk GaAs was reported in numerous publications [2–8]. Most of these studies were carried out in the spectral range of 1 μm, which is above the band gap energy ($E_g = 1.42$ eV). Negative nonlinear refraction and strong nonlinear absorption were reported in these studies. Also reported was the observation of confinement effects in the case of nanocluster-shaped GaAs and thin GaAs films [9–11]. The values of nonlinear refractive indexes as high as $\gamma = -2.1 \times 10^{-6}$ cm^2 W^{-1} were measured close to the band gap energy of GaAs [12]. The nonlinear absorption in a heavily doped n-GaAs near the fundamental absorption edge was calculated in [7] on the basis of the model used in [13]. The transmission Z-scan technique commonly used for the determination of nonlinear optical parameters cannot be applied in the absorption range of the spectrum for a bulk GaAs crystal. The absorption in the visible range restricts the measurement of distortions in the transmitted beam, which will require a sample thickness that is near the absorption length. The reflection Z-scan technique [14, 15] can overcome some difficulties in the measurement of nonlinear optical characteristics of semiconductors at the photon energy $\hbar\omega > E_g$. This technique measures the nonlinear terms of susceptibility through the consequent changes in the reflection coefficient of the sample.

The chemical techniques for the preparation of GaAs nanoparticles were discussed by Malik et al. [16]. Laser ablation was also widely used for the preparation of GaAs nanoparticles on the surfaces of various materials. Laser ablation of GaAs was reported in various publications (see [17, 18] and references therein). Most of these studies were performed in vacuum conditions for the preparation of thin GaAs films. However, the application of laser ablation of GaAs in liquids and the analysis of structural, optical, and nonlinear optical properties of colloidal GaAs have not been reported so far, to the best of our knowledge. This technique has a number of advantages compared to ion implantation in solids (simplicity, cost, variability, etc). Meanwhile, this technique can be applied for the preparation of colloidal semiconductor solutions [19, 20]. High nonlinear optical susceptibilities ($\sim 10^{-8}$ esu) of such nanoparticles were attributed to quantum confinement effects.

Quantum confinement is attributed to the small-size effect, which alters the electronic structures of nanocrystals from those of the bulk materials. This effect has been extensively studied due to scientific interest and technical importance. The third-order optical nonlinearity of confined GaAs quantum dots was predicted to be significantly higher compared to bulk GaAs [21]. It was shown that the nonlinear refractive index of GaAs-doped glasses at 1,060 nm ($\gamma = -5.6 \times 10^{-12}$ cm^2 W) is over an order of magnitude greater than that of bulk GaAs ($\gamma = -4.1 \times 10^{-13}$ cm^2 W). Justus et al. have shown that the two-photon absorption coefficient of a GaAs-doped glass composite is similar to that of bulk GaAs ($\beta = 26 \times 10^{-9}$ cm W^{-1}), thus, indicating that the nonlinear absorption coefficient is enhancing in the quantum-confined

✉ E-mail: r_ganeev@issp.u-tokyo.ac.jp

sample [9]. An interest in the synthesis, characterization, and application of colloidal semiconductor "quantum dot" materials has grown markedly since these studies are aimed to bridge the gap between solids and atoms. This increased attention reflects both the strong size dependence of optical and electronic properties of these materials, and the fact that the materials are relatively easy to make with well controlled particle sizes. However, the dependence of the optical nonlinearities on the sizes of the semiconductor nanoparticles has yet to be determined.

In this paper, we present the results of the studies of optical, structural, and nonlinear optical properties of GaAs nanoparticles prepared by laser ablation in various liquids. We analyze the nonlinear refraction and nonlinear absorption of these media using the radiation of different pulse repetition rates, pulse durations, and wavelengths.

2 Experimental arrangements

Laser ablation of GaAs in liquids was carried out using second-harmonic radiation of an Nd:YAG laser (Spectra-Physics, LAB 150). Laser radiation (wavelength $\lambda = 532$ nm, pulse duration $t = 9$ ns, pulse energy $E = 30$ mJ, 10 Hz pulse repetition rate) was focused by a 50-mm focal length lens at normal incidence onto the surface of a GaAs wafer placed inside the 10-mm thick cell filled with liquids of different viscosity (water, ethanol, ethylene glycol, or silicon oil). The fluence of the 532-nm radiation at the target surface was measured to be 20 J cm^{-2}. The ablation was carried out during 15–45 min. The solution was constantly stirred during the interaction of the laser radiation with the GaAs target to prevent the increase of concentration of GaAs nanoparticles in front of the ablated area. The prepared solutions were analyzed by transmission electron microscope (TEM) and spectroscopic techniques to confirm the appearance of GaAs nanoparticles. The volume ratio of GaAs in the liquid solutions was estimated to be $\sim 2 \times 10^{-4}$.

The GaAs solutions were then studied using the Z-scan technique [22] to measure their nonlinear optical characteristics. The 1, 2, 5, and 10-mm-thick silica glass cells filled with the investigated solutions were used for these studies. The laser radiation was focused by 200, 400, or 800-mm focal length lenses. The samples were moved along the z-axis through the focal area to observe the variations of the phase and amplitude of the propagated radiation in the far field. The energy of the laser pulses was measured by a calibrated photodiode. A 1-mm long aperture was placed at the distance of 500 mm from the focal plane (closed-aperture scheme). The radiation propagated through this aperture was registered by a second photodiode. The closed-aperture scheme allowed the determining of both the sign and the value of the nonlinear refractive index of the samples. The open-aperture scheme was used in order to determine the value of the nonlinear absorption coefficient. A charge coupled device (CCD) camera was used for the analysis of the variations of the spatial shapes of the radiation propagated through the samples in the Z-scan-like scheme. A detailed description of the experimental setup can be found elsewhere [23].

Various lasers operating at different lasing conditions were used in these Z-scan studies. The first one was the Ti:sapphire laser (Spectra-Physics, Tsunami + CPA TSA-10F) delivering a femtosecond radiation operating at a 10-Hz pulse repetition rate ($t = 110$ fs, $\lambda = 795$ nm, $E = 10$ mJ). The output radiation and its second harmonic with variable pulse duration were also available from this laser. The laser also operated at a Q-switched regime delivering 8-ns pulses. The 795-nm, 80-MHz, 100-fs, 300-mW pulses from the seeding oscillator (Tsunami) were used for the investigation of thermal-effect-induced self-interaction in the solutions. We also used the 1,054-nm, 100-MHz, 280-fs, 100-mW radiation (Time Bandwidth, GLX-200) for the investigation of thermal-effect-induced nonlinear optical processes caused by infrared (IR) radiation.

3 Results and discussion

3.1 *Optical and structural characteristics of GaAs*

The appearance of stable GaAs nanoparticles in our studies was confirmed by the TEM studies of these solutions. The analysis of the nanoparticles' sizes was carried out using transmission electron microscope JEM-201OF. A drop of the GaAs-containing solution was placed on a carbon-coated copper grid that was left to dry before transferring into the TEM sample chamber. Figure 1 presents the TEM image of a GaAs nanoparticle in ethylene glycol (GaAs:EG). The TEM measurements conducted just after laser ablation have shown the appearance of nanoparticles with a size distribution ranging from 5 nm to 200 nm. This distribution was considerably narrowed after the sedimentation of long-sized nanoparticles with only small nanoparticles (ranging from 5 nm to 15 nm) dominating the GaAs solution. The spacing of 0.32 nm was exhibited in the high-resolution TEM micrographs, which corresponds to the d (111) of a GaAs zinc-blend structure, analogous to those reported in [18]. The nanoparticles tend to aggregate in the selected areas on the TEM grid, so we could not estimate the total size distribution with certainty. An elemental analysis of GaAs nanoparticles using energy dispersive X-ray spectroscopy also confirmed the presence of GaAs in the solutions (Fig. 2; the copper and carbon lines originate from the grid material). These studies have shown that the particles tend to be gallium-rich (the accounted weight ratio Ga:As $\sim$ 1.4:1), which was higher compared to other reported values (1.2:1 [16, 24]).

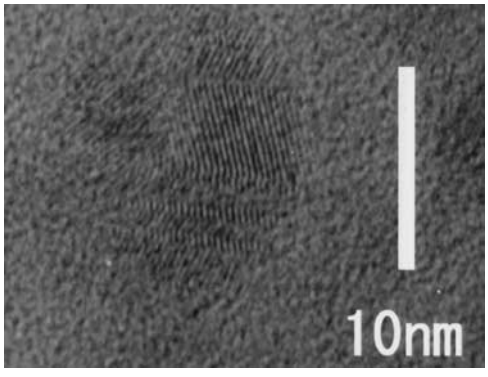

FIGURE 1 Transmission electron microscope (TEM) micrograph of a single GaAs nanoparticle from the GaAs:EG solution

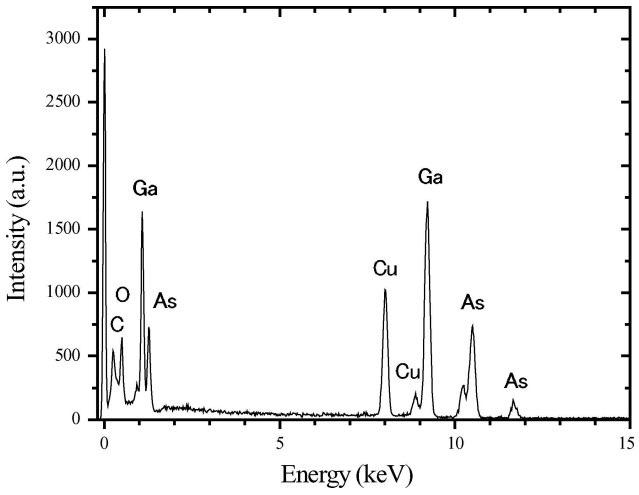

FIGURE 2 The energy dispersive X-ray spectrum of the GaAs:ethanol solution

The absorption spectra of solutions were similar to those of quantum-confined GaAs nanocrystals embedded in glasses [9], exhibiting a broad absorption through the visible and ultraviolet (UV) ranges. Figure 3, curve 1 shows the absorption spectrum of GaAs deposited in ethylene glycol. The absorption curve was considerably blue-shifted compared to the bulk GaAs (curve 5). The linear absorption coefficients of GaAs-nanoparticles-contained ethylene glycol at 397 nm and 795 nm were measured to be 1.6 cm^{-1} and 0.35 cm^{-1}, respectively. The effect of liquid degradation inside the focal volume where the formation of nanoparticles takes place was negligible in the case of water, ethanol, and ethylene glycol, since our observations of silver ablation in analogous conditions have shown an absorption spectrum that can be attributed to the surface plasmon resonance of silver (Fig. 3, curve 3). However, in the case of silicon oil, we observed its degradation in both of these cases.

The variations of the absorption spectra of GaAs nanoparticles in water, ethylene glycol, and ethanol caused by sedimentation of long nanoparticles were observed during a period of one month (Fig. 3, curves 1 and 2). In the case of GaAs ablated in silicon oil (GaAs:SO) the nanoparticle size distribution and absorption spectra remained constant due to the high viscosity of the host material. In that case, we observed an inhomogeneous distribution of GaAs particles ranging from big blocks (0.2–10 μm) to nanoparticle-sized structures.

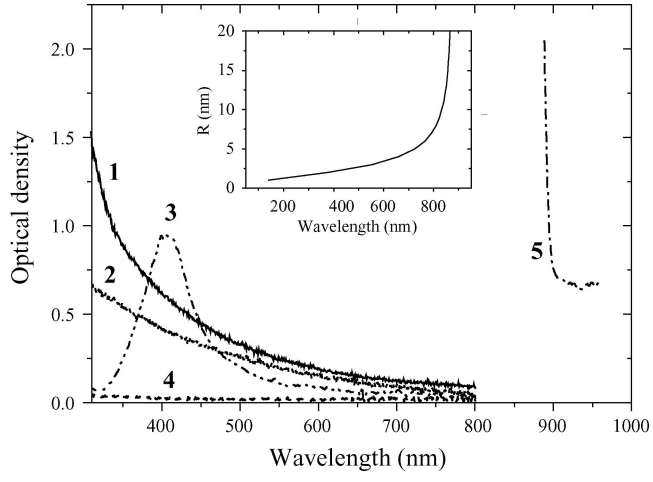

FIGURE 3 The absorption spectra of 10-mm thick GaAs:EG solution (1) 1 and (2) 3 weeks after ablation, (3) silver:EG solution, (4) pure ethylene glycol, and (5) 500-μm thick bulk GaAs wafer. *Inset*: the calculated dependence of the band gap wavelength on the radius of the GaAs nanoparticles

There were some previous reports indicating that the absorption spectra of large semiconductor nanoparticles appear to be the same as the ones of bulk semiconductors. In particular, the laser ablation was applied for the preparation of CdS and ZnSe colloidal solutions, and it was shown that there were no considerable distinctions in the absorption spectra of nanoparticle solutions and bulk crystals [19]. However, for nanoparticles with sizes smaller than the Bohr radius of an exciton, a considerable blue shift in the absorption spectra caused by the quantum confinement effect is a common feature. The blue shift in the absorption spectra of small GaAs nanoparticles was reported in [16]. In particular, the absorption edges of nanoparticles with a diameter of 4.47 nm and 5.45 nm were located at 494 nm and 580 nm, respectively. In our case, we did not observe the fixed absorption edge for GaAs solutions due to the presence of nanoparticles of different sizes. The band gap shift in that case was undefined; it appeared as a featureless absorption curve.

When the radius of the semiconductor nanoparticles becomes close to or smaller than the Bohr radius of an exciton, then their optical properties can be altered. The the radius of a Bohr exciton can be calculated by:

$$R_{\mathrm{b}} = \frac{4\pi\varepsilon_0\varepsilon\hbar^2}{e^2}\left(\frac{1}{m_{\mathrm{e}}} + \frac{1}{m_{\mathrm{h}}}\right) \tag{1}$$

Here, ε_0 and ε are the dielectric constants of the free space and the semiconductor ($\varepsilon = 12.8$ for GaAs), $\hbar$ is the Planck constant, m_{e} and m_{h} are the effective masses of the electron and the hole ($m_{\mathrm{e}} = 0.067m_0$ and $m_{\mathrm{h}} = 0.2m_0$ for GaAs, m_0 is the electron mass), and e is the charge of an electron. The value of R_{b} for GaAs was calculated to be 13.5 nm.

The change of band gap energy of the nanoparticles can be written as:

$$\Delta E_{\mathrm{g}} = \frac{\pi e R_{\mathrm{b}}}{8\varepsilon_0\varepsilon R^2} - \frac{1.786e^2}{4\pi\varepsilon_0\varepsilon R} \tag{2}$$

where R is the radius of the nanoparticles.

The dependence of the band gap wavelength on the radius of the GaAs nanoparticles is presented in the inset of Fig. 3. Using this dependence and the results of our spectral measurements, the average sizes of the GaAs nanoparticles were estimated to be in the range $R = 1.7$–8 HM, which was close to our TEM data.

The initial absorption spectra of GaAs ablated in different liquids (water, ethylene glycol, ethanol) were similar. However, after 2 weeks, the absorption of the GaAs:water and GaAs:ethanol solutions was weakened relative to GaAs:EG, probably due to the stronger viscosity in the latter case that led to the smaller rate of sedimentation.

It is worth noting the opportunity of using of the organic solvents instead of inorganic ones for various reasons. One of the advantages of preparing nanoparticles in organic solvents is that the distribution of particle sizes is narrower than that in water, as it was shown for polyvinylpyrrolydone solutions of CdS nanoparticles [25]. The stabilization of metal nanoparticle nonlinearities using polyvinylpyrrolydone stabilizers was shown in [26]. The nonlinear parameters of the semiconductor nanoparticle solutions in the case of organic solvents can be increased considerably due to the formation of clusters with controlled sizes.

3.2 *Investigations of nonlinear optical characteristics of GaAs nanoparticles*

The nonlinear optical properties of GaAs nanoparticles were previously studied using GaAs embedded in various glass matrices. Below, we present the results of our studies of nonlinear refraction and nonlinear absorption of GaAs nanoparticles deposited in various liquids.

The aggregation and sedimentation of GaAs nanoparticles caused the variations in their optical and nonlinear optical properties. We analyzed the nonlinear optical properties of GaAs-containing solutions mostly after the stabilization of their structural characteristics. The fresh colloids possessed by higher values of nonlinear optical parameters, however, caused these measurements to show poor reproducibility.

3.2.1 Nonlinear optical studies at high pulse repetition rate. Previously reported influence of thermal accumulative effects on nonlinear optical refraction in some media at high repetition rates of femtosecond pulses (of order of tens MHz [27]) has shown the importance of heat accumulation due to linear and/or nonlinear absorption. The first set of our nonlinear optical studies was carried out using the laser radiation of a high pulse repetition rate. We used the radiation of a Ti:sapphire oscillator ($\lambda = 795$ nm, $W = 300$ mW, $t = 100$ fs, 80-MHz pulse repetition rate) to analyze the influence of thermal-effect-induced nonlinearities on the propagation of laser radiation through the GaAs-containing solutions.

There are different mechanisms of losses of 795-nm radiation in these solutions. Among them, the single-photon scattering and absorption and the two-photon absorption seem to be the most important. However, the peak intensity of the laser radiation ($I_0 = 3 \times 10^9$ W cm^{-2}) and the small concentration were insufficient to cause the efficient nonlinear absorption in our experimental conditions.

The Z-scan studies using CCD images in the case of Kerr-induced nonlinearities were previously reported by Marcano et al. [28]. Here, we present the application of CCD images for the analysis of thermal-effect-induced self-defocusing. Figure 4 presents the beam shape variations in the far field in the case of a GaAs:EG solution using the Z-scan-like scheme. The arrows show the position of the 2-mm thick cell filled with GaAs:EG solution and the CCD images in the far field, respectively. A strong thermal-effect-induced self-defocusing caused by absorbed radiation is clearly seen in these images. At $z = z_1$ (CCD image No. 3), the self-defocusing caused by the thermal lens concentrates the radiation in the far field compared to the reference beam (No. 1). At $z = z_2$, the self-defocusing leads to the appearance of ring-shaped beam (No. 7). The z_1 and z_2 positions correspond to the peak and the valley of normalized transmittance in the case of closed-aperture measurements.

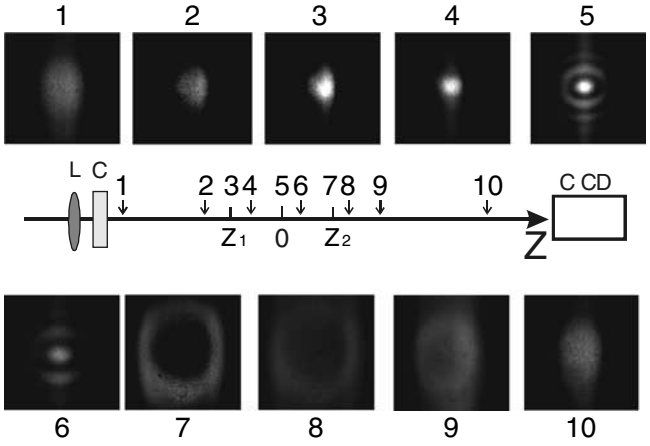

FIGURE 4 CCD images of the beam shapes of 795-nm radiation operated at a high pulse repetition rate and propagated through the GaAs:EG solution at the different positions of cells in a Z-scan-like scheme. *L*: focusing lens; *C*: silica glass cell filled with GaAs:EG solution; *CCD*: charge coupled device

The pure ethylene glycol has also shown the self-defocusing properties caused by thermal lens appearance due to nonlinear, probably three-photon, absorption of radiation. In that case, the thermal-effect-induced self-defocusing was considerably weaker in comparison with GaAs-nanoparticles-containing solution. Our observations have shown the insignificant influence of accumulative thermal effects on the variations of the refractive index in the cases of pure water and ethanol.

The difference in the absorption mechanisms leading to the negative nonlinear refraction was clearly seen from the Z-scans of GaAs:EG and pure ethylene glycol. Figure 5a presents two Z-scan curves measured using the 1-mm thick cells filled with GaAs:EG (filled squares) and pure ethylene glycol (open circles). The linear absorption is responsible for the observed nonlinear refraction in the case of the GaAs:EG solution ($\Delta Z_{\mathrm{pv}} = 3.5$ mm $\approx 1.7 z_0$), whereas in the case of pure ethylene glycol, the nonlinear absorption is the main mechanism of thermal-effect-induced nonlinearity ($\Delta Z_{\mathrm{pv}} = 2.5\,\mathrm{mm} \approx 1.2 z_0$). Here, $z_0 = \pi w_0^2/\lambda = 2$ mm is the diffraction length of the focused beam and w_0 is the beam waist radius. Analogous measurements were performed using the GaAs:SO solution (Fig. 5b).

The nonlinear refractive coefficient of ethylene glycol can be easily extracted from our measurements (Fig. 5a), taking into account a standard technique of calculation reported in [22]. This value is found to be $\gamma = -6.3 \times 10^{-14}$ cm^2 W^{-1}. The thermal-effect-induced nonlinear refractive index of the GaAs:EG solution extracted from the same data presented in Fig. 5a was measured to be $\gamma = -4 \times 10^{-13}$ cm^2 W^{-1}, taking into account the experimental conditions of these experiments. Both these data sets represent the influence of slow nonlinear processes.

The similar variations of the beam shape in the case of 1,054-nm, 280-fs, 100-MHz, 100-mW radiation propagated

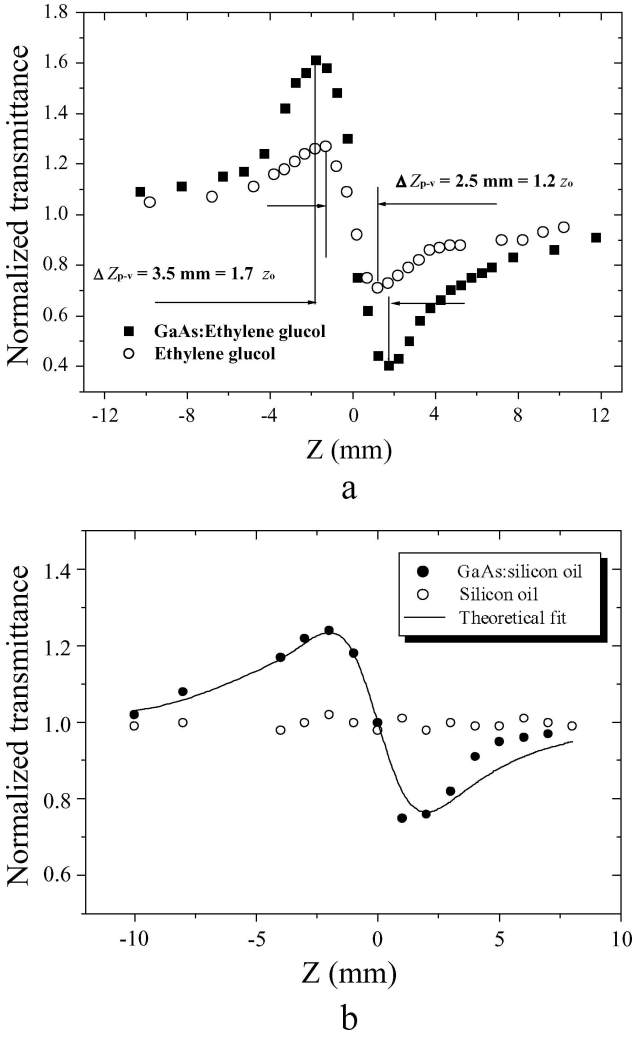

FIGURE 5 **a** The Z-scan curves measured using the 1-mm thick cells filled with GaAs:EG (*filled squares*) and pure EG (*open circles*) at different average powers of 795-nm radiation. **b** Analogous measurements using GaAs:SO and pure silicon oil

through the GaAs-containing solutions confirmed a decisive role of linear absorption (Fig. 6). No absorption and beam shape variations were observed at $\lambda = 1,054$ nm in the case of pure ethylene glycol, ethanol, and water.

3.2.2 Low pulse repetition rate. In the next set of nonlinear optical studies, we used the radiation operated at a 10-Hz pulse repetition rate in order to exclude the influence of slow thermal accumulative processes observed at high pulse repetition rates. In the case of nanosecond pulses ($\lambda = 795$ nm, $t = 8$ ns, 10-Hz pulse repetition rate), we did not observe the fast Kerr-induced nonlinear optical processes in GaAs-containing solutions up to maximum intensities leading to the optical breakdown of the surface of silica glass cells at this pulse duration ($I_0 = 8 \times 10^9$ W cm^{-2}). These studies were carried out using the closed-aperture Z-scans and time-integrated photodiodes. However, the self-defocusing was observed when we analyzed the time waveform of the propagated pulses using fast p-i-n diodes. A detailed description of this technique is presented in [29]. The idea of this technique is based on the analysis of the oscilloscope traces of the pulse propagated through the nonlinear medium in a closed-aperture Z-scan scheme.

We observed a suppression of the trailing part of the pulse when the samples were placed at $z = z_2$. Such variation of a temporal waveform shows the influence of self-defocusing in the investigated medium. Analogous observations were previously reported in various liquid-containing media (methyl nitroaniline solutions [30], aqueous colloidal metals [31], CS_2 [29]). The origin of the observed self-interaction process is a thermal-effect-induced negative lens appearance due to the absorption of part of the laser radiation. However, this process was caused by mechanisms other than those observed in the case of a high pulse repetition rate. In the latter case, the appearance of a negative lens was caused by heat accumulation, whereas in the former case, the self-defocusing was caused by acoustic wave propagation through the beam waist area. The acoustic wave was generated as a result of the optical absorption of laser radiation.

Next, we discuss the thermal-effect-induced self-interaction process observed in the case of nanosecond pulses. The thermal lens appears with energy absorption growth. This lensing is more effective for the trailing part of the pulse

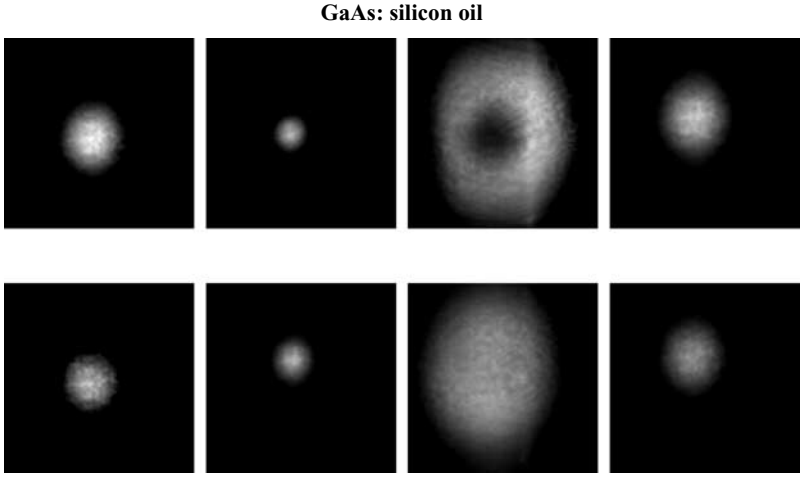

FIGURE 6 CCD images of the beam shapes of 1,054-nm radiation operated at high pulse repetition rates and propagated through the GaAs:SO and GaAs:EG solutions at different positions of cells in a Z-scan-like configuration. Positions 1–4 correspond to Nos. 1, 3, 7, and 10 cell positions presented in Fig. 4

because of the time delay of this process due to the transfer of energy to the solvent and the temperature rise of the solution. The heating of the host dielectric has a rise-time consisting of the time t_1 required for energy transfer from the nanoparticles to the solvent and time t_2 required for the temperature rise of the solvent to be transformed into the change of refractive index via density reduction. t_1 is a function of the nanoparticles' sizes. For 10-nm particles, this time is of the order of 25 ps. t_2 is equal to w_0/υ, where υ is the velocity of an acoustic wave in liquid. In our case, ($w_0 = 21\,\mu$m, $\upsilon = 1,500$ m/s), this parameter is equal to $t_2 = 14$ ns. It means that, at least for the central part of the focused beam, there are some conditions of self-defocusing in the GaAs solution during propagation of the nanosecond radiation through the sample. It takes between 4 ns and 6 ns to achieve the density variations in the central part of the focal volume. These estimations of the self-defocusing start-up time are qualitatively coinciding with experimental observations of the variations of the trailing part of 8-ns pulses in a closed-aperture scheme.

The application of short laser pulses (in the picosecond and femtosecond ranges) at low pulse repetition rates allows the exclusion of the influence of slow thermal-related nonlinear optical processes and the analysis of the self-interaction mechanisms caused by the electronic response of GaAs nanoparticles. The femtosecond continuum was generated in GaAs-containing liquids in the case of the shortest femtosecond pulses. We carried out our studies in the conditions when no white light was observed in order to exclude the influence of phase variations caused by self-phase modulation of ultrashort pulses in liquid media.

Our studies using the 795-nm and 397-nm femtosecond radiations were performed at laser intensities up to $I_0 = 1 \times 10^{11}$ W cm^{-2}. We did not register the influence of GaAs nanoparticles on the nonlinear refractive properties of the GaAs:liquid solutions. The influence of the positive refractive nonlinearities of the silica glass and water was observed at the intensities exceeding 4×10^{10} W cm^{-2} ($\lambda = 795$ nm), which eclipsed the influence of the GaAs nanoparticles. The only nonlinear optical process observed at 795 nm in GaAs-nanoparticles-containing liquids was a nonlinear absorption due to two-photon processes in these compounds (Fig. 7).

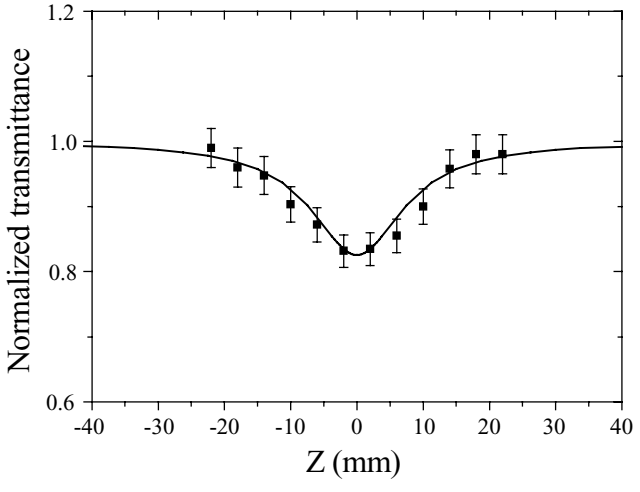

FIGURE 7 Normalized transmittance of the GaAs:water solution in an open-aperture Z-scan. The *solid line* shows theoretical fit

The normalized transmittance in the case of an open-aperture scheme can be determined as [22]:

$$T(z) = \sum_{m=0}^{\infty} \frac{[-q_0(z)]^m}{(m+1)^{3/2}} \quad \text{for} \quad |q_0| < 1 \tag{3}$$

where:

$$q_0 = \beta \frac{I_0[1 - \exp(-\alpha L)]}{[1 + (z/z_0)^2]\alpha} \tag{4}$$

α is the linear absorption coefficient, and L is the length of the nonlinear medium. After the fitting of Eq. 3 with experimental data (Fig. 7, solid curve), the nonlinear absorption coefficient of the GaAs:water solution was calculated to be 0.7×10^{-9} cm W^{-1}. This value was only 30–40 times below the one measured in bulk GaAs in IR range (26×10^{-9} cm W^{-1}), in spite of the small volume ratio of the GaAs in liquid solutions ($\sim 2 \times 10^{-4}$), thus, indicating the influence of quantum confinement on the enhancement of β of a GaAs nanoparticles solution. We estimated the third-order susceptibility of GaAs nanoparticles at 795 nm to be $|\chi^{(3)}| \sim 2 \times 10^{-9}$ esu, assuming the volume ratio of GaAs nanoparticles. Analogous nonlinearities were reported previously for As_2S_3 and CdS nanoparticles solutions [32].

We observed a variation of normalized transmittance in an open-aperture scheme in the case of 795-nm, 400-fs pulses operated at a 10-Hz repetition rate. This regime of laser–colloids interaction at high irradiation leads to the fragmentation of GaAs nanoparticles. As a result, a nonlinear absorption presented by a normalized $T(z)$ dependence was less pronounced in the case of a 10-Hz pulse repetition rate compared to a single-shot interaction. These measurements were repeated several times to ensure reproducibility, and were also performed in pure liquid-containing cells, which showed no measurable nonlinear response under the same conditions.

The "cost" of laser ablation as a simpler preparation method in terms of properties is short-term stability. This is a main obstacle of this technique. It would be problematic for technological applications of the material in the case when optical properties of a nonlinear device containing such structures appear to be unstable under long-term laser irradiation. One of the possible proposals to overcome this obstacle is the preparation of semiconductor nanoparticles contained in a solution using low viscosity liquid and further dissolution of a prepared solution in the matrix with a high viscosity. For example, the GaAs:ethanol solution could be dissolved in silicon oil with further evaporation of ethanol.

Finally, we briefly discuss the application of GaAs-containing liquids as optical limiters. Investigation of optical limiting in various materials opens new opportunities for their application as laser switching systems for protection from intense laser radiation.

We studied the optical limiting processes in GaAs-containing liquids using subpicosecond radiation. The laser radiation was focused by a 100-mm focal length lens inside the 10-mm thick cells containing colloidal GaAs. The transmitted radiation was measured by a calibrated photodiode. Figure 8 presents the normalized transmittance dependencies as functions of the pulse energy in the case of GaAs:EG and GaAs:water solutions and pure water. Optical limiting in

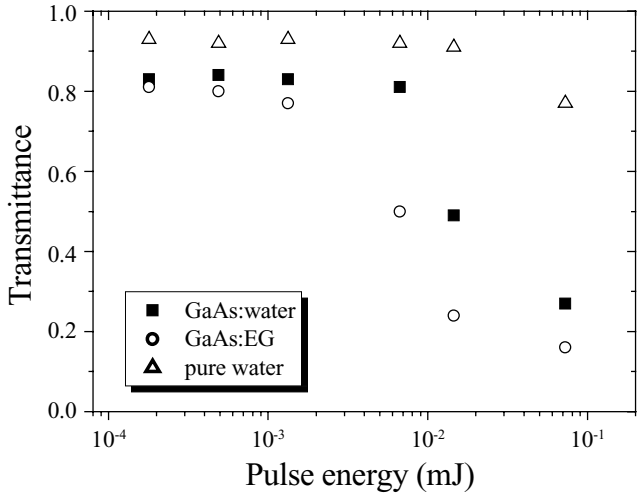

FIGURE 8 Normalized transmittance dependencies as functions of laser radiation energy in the case of GaAs:EG and GaAs:water solutions and pure water

the solutions was observed at the pulse energies exceeding (5–8) $\times 10^{-6}$ J, and was caused by two-photon absorption, which was confirmed by nonlinear absorption investigations using an open-aperture Z-scan scheme. We observed the influence of white light generation in pure water at pulse energy 8×10^{-5} J and pulse duration $t = 900$ fs.

Our recent studies of silver nanoparticles in various liquids prepared by the same technique of laser ablation [33] have revealed identical properties compared to those reported in this paper. The viscosity of the liquids plays an important role in preserving the optical and nonlinear optical characteristics of the nanoparticles solutions in both cases. The intensity thresholds of femtosecond continuum generation both in Ag- and GaAs-containing solutions were higher than those for pure liquids. The thermal-lens-induced self-defocusing dominated in these solutions in the case of high pulse repetition rates. However, the appearance of a strong absorption band in silver-nanoparticles-containing solutions at ∼400 nm associated with surface plasmon resonance was responsible for the enhancement of fast nonlinear optical processes (two-photon absorption, saturable absorption, and Kerr-induced self-defocusing) in the vicinity of this spectral range. None of these such features were registered in the case of GaAs solutions possessing by a featureless absorption spectrum.

4 Conclusions

In conclusion, we investigated the optical and structural properties as well as nonlinear refraction and absorption of GaAs nanoparticles prepared by laser ablation in various liquids. A drawback of laser-assisted deposition of GaAs in liquids was a very large distribution at the initial stages after ablation, followed by sedimentation of large-sized nanoparticles. The most important distinction between the investigated liquids, as host materials of GaAs nanoparticles, was caused by a difference in viscosity of these liquids that led to the stabilization of structural and nonlinear optical properties of the GaAs:EG solution for a longer period compared to GaAs:water and GaAs:ethanol solutions, where we observed considerable sedimentation.

We analyzed the self-defocusing effects in these solutions using the images of a beam transmitted by a charge coupled device (CCD) camera in a Z-scan-like scheme. Thermal-effect-induced self-defocusing processes dominated in the case of high pulse repetition rates, as well as in the case of nanosecond pulses. In the case of short laser pulses, two-photon absorption was observed in these colloidal solutions ($\beta = 0.7 \times 10^{-9}$ cm W^{-1}). We estimated the third-order susceptibility of GaAs nanoparticles at 795 nm, assuming a small volume ratio of GaAs in liquid solutions ($\sim 2 \times 10^{-4}$) to be $|\chi^{(3)}| \sim 2 \times 10^{-9}$ esu. The optical limiting properties of the GaAs-contained solutions were discussed.

REFERENCES

1 H. Ma, A.S.L. Gomes, C.B. de Araujo, Opt. Lett. **18**, 414 (1993)
2 D. Bethune, A.J. Schmidt, Y.R. Shen, Phys. Rev. B **11**, 3867 (1975)
3 M. Sheik-Bahae, D.C. Hutchings, D.J. Hagan, E.W. Van Stryland, IEEE J. Quantum Electron. **27**, 1296 (1991)
4 A. Agnessi, G.P. Banfi, M. Ghigliazza, G.C. Reali, Opt. Commun. **92**, 300 (1992)
5 Y.H. Lee, A. Chavez-Pirson, S.W. Koch, H.M. Gibbs, S.H. Park, J. Morhange, A. Jeffery, N. Peyghambarian, L. Banyai, A.C. Gossard, W. Wiegmann, Phys. Rev. Lett. **57**, 2446 (1986)
6 M.J. Lederer, B. Luther-Davies, H.H. Tan, C. Jagadish, M. Haiml, U. Siegner, U. Keller, Appl. Phys. Lett. **74**, 1993 (1999)
7 V.L. Malevich, I.A. Utkin, Semiconductors **34**, 924 (2000)
8 T. Skauli, P.S. Kuo, K.L. Vodopyanov, T.J. Pinguet, O. Levi, L.A. Eyres, J.S. Harris, M.M. Fejer, B. Gerard, L. Becouarn, E. Lallier, J. Appl. Phys. **94**, 6447 (2003)
9 B.L. Justus, R.J. Tonucci, A.D. Berry, Appl. Phys. Lett. **61**, 3151 (1992)
10 K. Akiyama, N. Tomita, Y. Nomura, T. Isu, Physica B **272**, 505 (1999)
11 M. Inoue, Jpn. J. Appl. Phys. **39**, 3971 (2000)
12 H.-C. Lee, A. Kost, M. Kawase, A. Hariz, P.D. Dapkus, E.M. Garmire, IEEE J. Quantum Electron. **24**, 1581 (1988)
13 S.W. Koch, S. Schmidt-Rink, H. Haug, Phys. Status Solidi b **106**, 135 (1981)
14 D.V. Petrov, A.S.L. Gomes, C.B. de Araujo, Appl. Phys. Lett. **65**, 1067 (1994)
15 M. Martinelli, L. Gomes, R.J. Horowicz, Appl. Opt. **39**, 6193 (2000)
16 M.A. Malik, P. O'Brien, S. Norager, J. Smith, J. Mater. Chem. **13**, 2591 (2003)
17 J. Perriere, E. Millon, M. Chamarro, M. Morcrette, C. Andreazza, Appl. Phys. Lett. **78**, 2949 (2001)
18 A. Borowiec, M. Mackenzie, G.C. Weatherly, H.K. Haugen, Appl. Phys. A **77**, 411 (2003)
19 K.V. Anikin, N.N. Melnik, A.V. Simakin, G.A. Shafeev, V.V. Voronov, A.G. Vitukhnovsky, Chem. Phys. Lett. **336**, 357 (2002)
20 R.A. Ganeev, A.I. Ryasnyansky, T. Usmanov, Opt. Quantum Elecrton. **35**, 211 (2003)
21 L. Banyai, M. Lindberg, S.W. Koch, Opt. Lett. **13**, 212 (1988)
22 M. Sheik-Bahae, A.A. Said, T.-H. Wei, D.J. Hagan, E.W. Van Stryland, IEEE J. Quantum Electron. **26**, 760 (1990)
23 R.A. Ganeev, M. Baba, A.I. Ryasnyansky, M. Suzuki, M. Turu, H. Kuroda, Opt. Commun. **231**, 431 (2004)
24 S.S. Kher, R.L. Wells, Chem. Mater. **6**, 2056 (1994)
25 H. Yao, S. Takahara, H. Mizuma, T. Kosegi, T. Hayashi, Jpn. J. Appl. Phys. **35**, 4633 (1996)
26 R.A. Ganeev, A.I. Ryasnyansky, M.K. Kodirov, S.R. Kamalov, V.A. Li, R.A. Tugushev, T. Usmanov, Appl. Phys. B **74**, 47 (2002)
27 M. Falkonieri, G. Salvetti, Appl. Phys. B **69**, 133 (1999)
28 A. Markano, O.H. Maillotte, D. Gindre, D. Metin, Opt. Lett. **21**, 101 (1996)
29 R.A. Ganeev, M. Baba, A.I. Ryasnyansky, M. Suzuki, M. Turu, H. Kuroda, Appl. Phys. B **78**, 433 (2004)
30 H. Toda, C.M. Verber, Opt. Lett. **17**, 1379 (1992)
31 R.A. Ganeev, A.I. Ryasnyansky, S.R. Kamalov, M.K. Kodirov, T. Usmanov, J. Phys. D: Appl. Phys. **34**, 1602 (2001)
32 R.A. Ganeev, A.I. Ryasnyansky, R.I. Tugushev, T. Usmanov, J. Opt. A **5**, 409 (2003)
33 R.A. Ganeev, M. Baba, A.I. Ryasnyansky, M. Suzuki, H. Kuroda, Opt. Commun. **240**, 437 (2004)